ELECTROCARDIOGRAM (ECG) SIGNAL PROCESSING

LEIF SÖRNMO
Lund University
Sweden
PABLO LAGUNA
Zaragoza University
Spain

1. INTRODUCTION

Signal processing today is performed in the vast majority of systems for ECG analysis and interpretation. The objective of ECG signal processing is manifold and comprises the improvement of measurement accuracy and reproducibility (when compared with manual measurements) and the extraction of information not readily available from the signal through visual assessment. In many situations, the ECG is recorded during ambulatory or strenuous conditions such that the signal is corrupted by different types of noise, sometimes originating from another physiological process of the body. Hence, noise reduction represents another important objective of ECG signal processing; in fact, the waveforms of interest are sometimes so heavily masked by noise that their presence can only be revealed once appropriate signal processing has first been applied.

Electrocardiographic signals may be recorded on a long timescale (i.e., several days) for the purpose of identifying intermittently occurring disturbances in the heart rhythm. As a result, the produced ECG recording amounts to huge data sizes that quickly fill up available storage space. Transmission of signals across public telephone networks is another application in which large amounts of data are involved. For both situations, data compression is an essential operation and, consequently, represents yet another objective of ECG signal processing.

Signal processing has contributed significantly to a new understanding of the ECG and its dynamic properties as expressed by changes in rhythm and beat morphology. For example, techniques have been developed that characterize oscillations related to the cardiovascular system and reflected by subtle variations in heart rate. The detection of low-level, alternating changes in T wave amplitude is another example of oscillatory behavior that has been established as an indicator of increased risk for sudden, life-threatening arrhythmias. Neither of these two oscillatory signal properties can be perceived by the naked eye from a standard ECG printout.

Common to all types of ECG analysis—whether it concerns resting ECG interpretation, stress testing, ambulatory monitoring, or intensive care monitoring—is a basic set of algorithms that condition the signal with respect to different types of noise and artifacts, detect heartbeats, extract basic ECG measurements of wave amplitudes and durations, and compress the data for efficient storage or transmission; the block diagram in Fig. 1 presents this set of signal processing algorithms. Although these algorithms are frequently implemented to operate in sequential order, information on the occurrence time of a heartbeat, as produced by the QRS detector, is sometimes incorporated into the other algorithms to improve performance. The complexity of each algorithm varies from application to application so that, for example, noise filtering performed in ambulatory monitoring is much more sophisticated than that required in resting ECG analysis.

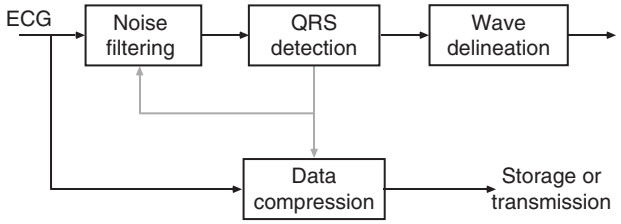

Figure 1. Algorithms for basic ECG signal processing. The timing information produced by the QRS detector may be fed to the blocks for noise filtering and data compression (indicated by gray arrows) to improve their respective performance. The output of the upper branch is the conditioned ECG signal and related temporal information, including the occurrence time of each heartbeat and the onset and end of each wave.

Once the information produced by the basic set of algorithms is available, a wide range of ECG applications exist where it is of interest to use signal processing for quantifying heart rhythm and beat morphology properties. The signal processing associated with two such applications—high-resolution ECG and T wave alternans—are briefly described at the end of this article. The interested reader is referred to, for example, Ref. 1, where a detailed description of other ECG applications can be found.

2. ECG PREPROCESSING

Considerable attention has been paid to the design of filters for the purpose of removing baseline wander and powerline interference; both types of disturbance imply the design of a narrowband filter. Removal of noise because of muscle activity represents another important filtering problem being much more difficult to handle because of the substantial spectral overlap between the ECG and muscle noise. Muscle noise present in the ECG can, however, be reduced whenever it is appropriate to employ techniques that benefit from the fact that the ECG is a recurrent signal. For example, ensemble averaging techniques can be successfully applied to time-aligned heartbeats for reduction of muscle noise.

The filtering techniques are primarily used for preprocessing of the signal and have as such been implemented in a wide variety of systems for ECG analysis. It should be remembered that filtering of the ECG is contextual and should be performed only when the desired information remains undistorted. This important insight may be exemplified by filtering for the removal of powerline interference. Such filtering is suitable in a system for the analysis of heart rate variability, whereas it is inappropri-

ate in a system for the analysis of micropotentials, as such potentials spectrally overlap the powerline interference.

2.1. Baseline Wander

Removal of baseline wander is required in order to minimize changes in beat morphology that do not have cardiac origin, which is especially important when subtle changes in the "low-frequency" ST segment are analyzed for the diagnosis of ischemia, which may be observed, for example, during the course of a stress test. The frequency content of baseline wander is usually in the range below 0.5 Hz; however, increased movement of the body during the latter stages of a stress test further increases the frequency content of baseline wander (see Fig. 2). Patients unable to perform a traditional treadmill or ergometer stress test may still be able to perform a stress test by either sitting, running an ergometer by hand, or using a special rowing device. In such cases, baseline wander related to motion of the arms severely distorts the ECG signal.

The design of a linear, time-invariant, highpass filter for removal of baseline wander involves several considerations, of which the most crucial are the choice of filter cut-off frequency and phase response characteristic. The cut-off frequency should obviously be chosen so that the clinical information in the ECG signal remains undistorted while as much as possible of the baseline wander is removed. Hence, it is essential to find the lowest frequency component of the ECG spectrum. In general, the slowest heart rate is considered to define this particular frequency component; the PQRST waveform is attributed to higher frequencies. During bradycardia, the heart rate may drop to approximately 40 beats/minute, implying that the lowest frequency contained in the ECG is approximately 0.67 Hz (2). As the heart rate is not perfectly regular but always fluctuates from one beat to the next, it is necessary to choose a slightly lower cut-off frequency such as 0.5 Hz. If too high a cut-off frequency is employed, the output of the highpass filter contains an unwanted, oscillatory component that is strongly correlated to the heart rate.

In certain situations, baseline wander becomes particularly pronounced at higher heart rates such as during the latter stages of a stress test when the workload increases. Then, it may be advantageous to couple the cut-off frequency to the prevailing heart rate, rather than to the lowest possible heart rate, to further improve baseline removal. Linear filtering with time-variable cut-off frequency was initially suggested for offline processing of ECG signals and later extended for online use (3,4).

The other crucial design consideration is related to the properties of the phase response and, consequently, the choice of filter structure. Linear phase filtering is highly desirable in order to prevent phase distortion from altering various wave properties of the cardiac cycle such as the duration of the QRS complex, the ST–T segment level, or the endpoint of the T wave. It is well-known that FIR filters can have an exact linear phase response, provided that the impulse response is either symmetric or antisymmetric; however, FIR designs result in high filter orders.

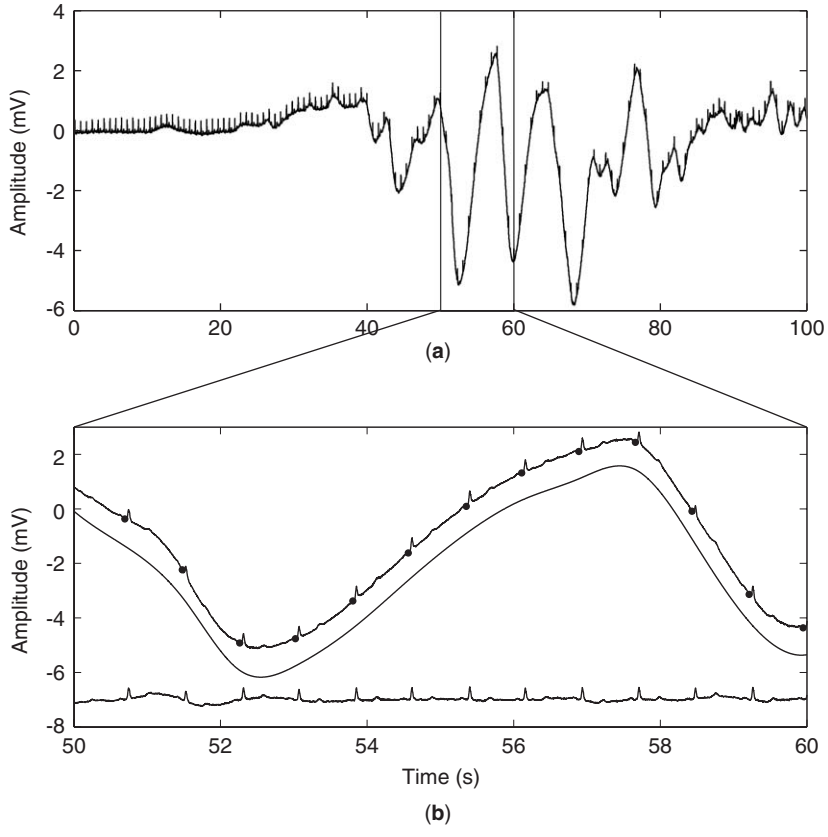

Figure 2. (a) Electrocardiographic baseline wander because of sudden body movements. The amplitude of the baseline wander is considerably larger than that of the QRS complexes. (b) A close-up in time (10 $\times$) of the ECG signal framed in (a), the estimated baseline obtained by fitting a cubic spline to the series of knots (indicated by dots), and the corrected ECG signal.

Forward-backward IIR filtering is a useful technique that exhibits the linear phase property. Although an IIR filter meets a magnitude specification more easily with a much lower filter order than does an FIR filter, it comes with a nonlinear phase response. The use of forward-backward filtering remedies this disadvantage because the overall result is filtering with a zero-phase transfer function. Implementation of such a filtering scheme involves three steps, namely, (1) processing of the input signal $x(n)$ with an IIR filter $h(n)$, (2) time reversal of the filter output, and repeated processing with $h(n)$, followed by (3) time reversal of the twice-filtered signal to produce the baseline-corrected output signal.

A useful low-complexity implementation of linear filtering involves sampling rate alteration (5). As the baseline wander to be removed is a narrowband component, filtering can be performed at a much lower sampling rate than at the rate of the original ECG signal. The main steps of this multirate approach are: (1) decimation of the original signal, which includes antialising filtering, to a lower sampling rate better suited to filtering, (2) lowpass filtering to produce an estimate of the baseline wander, (3) interpolation of the estimate back to the original sampling rate, and (4) subtraction of the estimate from the original ECG so as to produce the baseline-corrected signal. In addition to offering low complexity, the sampling rate alteration technique has the advantage of easily accommodating a time-variable cut-off frequency.

Yet another approach is to fit a polynomial to representative samples ("knots") of the ECG followed by subtraction of the polynomial. The fit is done by requiring the polynomial to pass through knots usually being selected within the isoelectric PQ segments. As the knots can only be located once QRS detection has been performed, the location of knots illustrates the feedback mechanism from QRS detection to noise filtering displayed in Fig. 1. Polynomial fitting can be interpreted as time-varying filtering in which the heart rate is controlling the cut-off frequency.

2.2. Powerline Interference

Electromagnetic fields caused by a powerline represent a common noise source in the ECG that is characterized by 50 or 60 Hz sinusoidal interference, possibly accompanied by a number of harmonics. Such narrowband noise renders the analysis and interpretation of the ECG more difficult, as the delineation of low-amplitude waveforms becomes unreliable and spurious waveforms may be introduced (6). Although various precautions can be taken to reduce the effect of powerline interference, for example, by selecting a recording location with few surrounding electrical devices or by appropriately shielding and grounding the location, it may still be necessary to perform signal processing to remove such interference. Several techniques have been presented for this purpose, ranging from straightforward linear, bandstop filtering to more advanced techniques that handle variations in powerline frequency and suppress the influence of transients manifested by the occurrence of QRS complexes (5,7).

A major concern when filtering out powerline interference is the degree to which the QRS complexes influence the output of the filter. The QRS complex acts, in fact, as an unwanted, large-amplitude impulse input to the filter. As linear, time-invariant notch filters are generally more sensitive to the presence of such impulses, powerline filters with a nonlinear structure may be preferable (8). In order to assure that a filter does not introduce unacceptable distortion, its performance should be assessed by means of simulated signals so that distortion can be exactly quantified.

3. QRS DETECTION

The presence of a heartbeat and its occurrence time is basic information required in all types of ECG signal processing. As the QRS complex is that waveform that is most easily discerned from the ECG, beat detection is synonymous to the detection of QRS complexes. The design of a QRS detector is of crucial importance because poor detection performance may propagate to subsequent processing steps and, consequently, limit the overall performance of the system. Beats that remain undetected constitute a more severe error than do false detections; the former type of error can be difficult to correct at a later stage in the chain of processing algorithms, whereas, hopefully, false detections can be eliminated by, for example, performing classification of QRS morphologies.

A QRS detector must be able to detect a large number of different QRS morphologies in order to be clinically useful and able to follow sudden or gradual changes of the prevailing QRS morphology. Furthermore, the detector must not lock onto certain types of rhythm, but treat the next possible event as if it could occur at almost any time after the most recently detected beat. Several detector-critical types of noise and artifacts exist depending on the ECG application of interest. The noise may be highly transient in nature or be of a more persistent nature, as exemplified by the presence of powerline interference. In the case of an ECG recording with episodes containing excessive noise, it may be necessary to exclude such episodes from further analysis. Figure 3 illustrates two types of noise that are particularly problematic in QRS detection.

Most detectors described in the literature have been developed from ad hoc reasoning and experimental insight. The general detector structure can be described by the block diagram in Fig. 4 (9,10). Within such a detector structure, the purpose of the preprocessor is to enhance the QRS complexes while suppressing noise and artifacts; the preprocessor is usually implemented as a linear filter followed by a nonlinear transformation. The output of the preprocessor is then fed to a decision rule for detection. The purpose of each processing block is summarized below.

The *linear filter* is designed to have bandpass characteristics such that the essential spectral content of the QRS complex is preserved, while unwanted ECG components such as the P and the T waves are suppressed (see Fig. 5). The center frequency of the filter varies from 10 to 25 Hz and the bandwidth from 5 to 10 Hz. In contrast to other types of ECG filtering, waveform distortion is not a

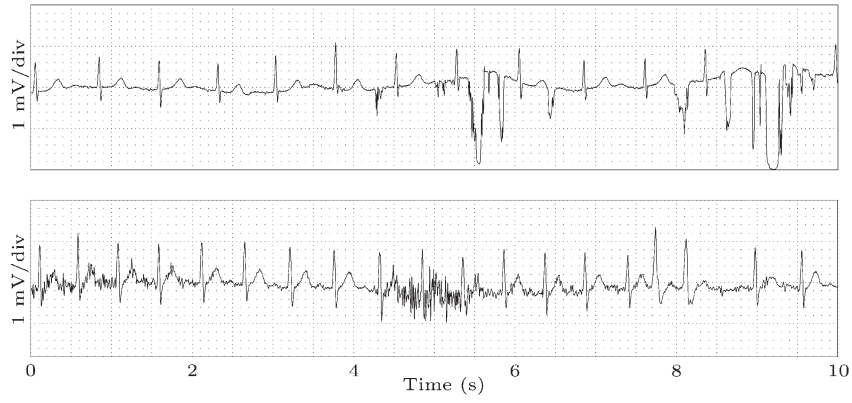

Figure 3. Examples of noise being problematic in QRS detection caused by electrode motion artifacts (top) and electromyographic noise (bottom).

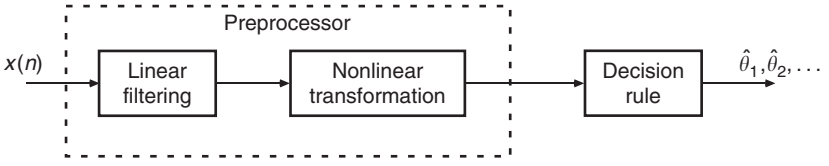

Figure 4. Block diagram of a commonly used QRS detector structure. The input is the ECG signal, and the output $\hat{\theta}_1, \hat{\theta}_2, \ldots$ is a series of occurrence times of the detected QRS complexes.

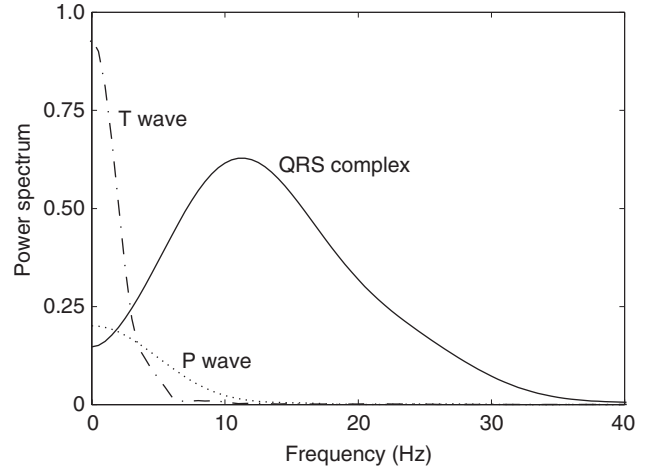

Figure 5. Power spectrum of the P wave, QRS complex, and T wave. The diagram serves as a rough guide to where the spectral components are located; large variations exist between beats of different lead, origin, and subjects.

critical issue in QRS detection. The focus is instead on improving the SNR to achieve good detector performance.

The *nonlinear transformation* further enhances the QRS complex in relation to the background noise as well as transforming each QRS complex into a single positive peak better suited for threshold detection. The transformation may consist of a memoryless operation, such as rectification or squaring of the bandpass-filtered signal, or a more complex transformation with memory. Not all preprocessors employ a nonlinear transformation, but the filtered signal is instead fed directly to the decision rule.

The *decision rule* takes the output of the preprocessor and performs a test on whether a QRS complex is present or not. The decision rule can be implemented as a simple amplitude threshold procedure, but usually include additional tests, for example, on reasonable waveform duration, to assure better immunity against various types of noise. The threshold is usually adapted to the most recent waveform amplitudes so that gradual changes in amplitude can be tracked.

It is interesting to note that the above detector structure can be derived from a model-based perspective by applying maximum likelihood estimation to a statistical model whose parameters describe the unknown occurrence time θ and amplitude a (5),

$$x(n) = as(n - \theta) + v(n). \tag{1}$$

In this model, the observed signal $x(n)$ is assumed to be composed of the waveform of interest, denoted $s(n)$, and additive noise $v(n)$, being a stationary, white Gaussian process. Although this model only accounts for a single heartbeat, the resulting detector structure can still be used to process successive intervals of the ECG signal.

Detector performance is commonly measured in terms of the probability of a true beat being detected, denoted P_D, and the probability of a false beat being detected P_F. The probability of a missed beat P_M is related to the probability of detection through $P_D = 1 - P_M$. These probabilities are usually estimated from the performance figures that results from analyzing a database of ECGs containing a large variety of QRS morphologies and noise types. The estimators are defined by ratios that include the number of correctly detected QRS complexes N_D, the number of false alarms N_F, and the number of missed beats N_M [i.e., $\hat{P}_F = N_F/(N_D + N_F)$ and $\hat{P}_D = N_D/(N_D + N_M)$]. As each probability is determined for each of the ECG recordings in the database, it is customary to compute a "gross" average of the estimates in order to reflect the overall performance of the QRS detector.

The numbers N_D, N_F, and N_M can only be computed once the database has been subjected to manual annotation. Such annotation is typically a laborious process, involving one or several skilled ECG readers, and leads

to every QRS complex being assigned its correct occurrence time θ_i. A beat is said to have been detected when the difference between the estimated occurrence time $\hat{\theta}_j$ and the annotation time θ_i is within a certain matching window defined by $\Delta\theta$. A false detection is produced when $\hat{\theta}_j$ is located at a distance larger than $\Delta\theta$ from any θ_i, and a beat is considered to have been missed when no detection occurs closer than $\Delta\theta$ to θ_i (Fig. 6).

As indicated by its name, the QRS detector is designed to detect heartbeats, while not producing occurrence times of the QRS complexes with high temporal resolution. Hence, it may be necessary to improve the resolution using an algorithm that performs time alignment of the detected beats. Such alignment reduces, for example, the problem of smearing that may occur when computing the ensemble average of several beats.

4. WAVE DELINEATION

Once the QRS complex has been detected, the T wave can be analyzed because ventricular repolarization always follows depolarization. Conversely, the P wave does not lend itself as easily to analysis because atrial and ventricular rhythms may be independent of each other. In the vast majority of cases, however, atrial and ventricular rhythms are associated so that P wave detection may be based on a backward search in time, beginning at the QRS complex and ending at the end of the preceding T wave.

A method of wave delineation determines the boundaries of each wave within the PQRST complex so that, with the resulting time instants, different wave durations can be computed (see Fig. 7). Once a wave has been delineated, other measures characterizing the wave, such as amplitude and morphology, can be easily computed. Such a method must also be able to detect when a certain wave is absent; this situation is commonly encountered because, for example, only the R wave or the S wave is present in certain leads or pathologies.

The classic definition of a wave boundary is the time instant at which the wave crosses a certain amplitude threshold level. Unfortunately, this definition is not well-suited for the common situation when the ECG contains baseline wander, and, therefore, this definition is rarely applied in practice. Instead, many methods for wave delineation exploit the change in slope that occurs at a boundary to avoid the problems because of low-frequency noise. Hence, the first derivative of the signal is calculated and analyzed with respect to zero crossings and extreme

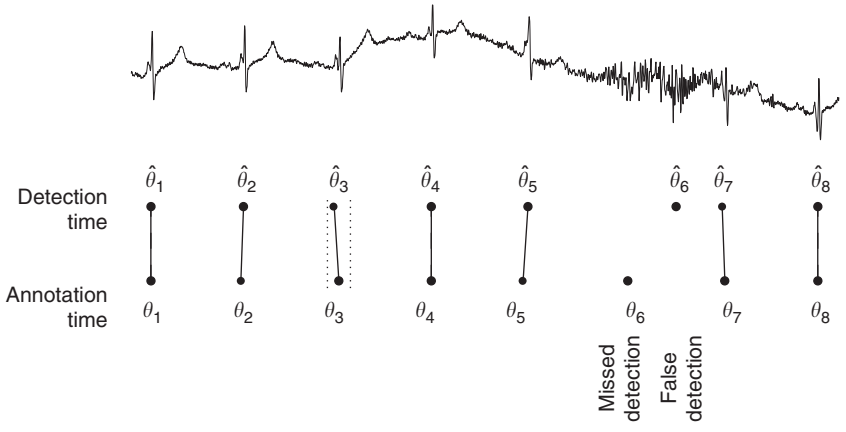

Figure 6. Comparison of the QRS detector output to the manual annotations, in this case indicating that all beats are correctly detected except the beat occurring at θ_6, which is missed. A noise wave is falsely detected at $\hat{\theta}_6$. The matching window, with length $\Delta\theta$, is displayed for the beat at θ_3 but is, of course, equally applicable to the other beats.

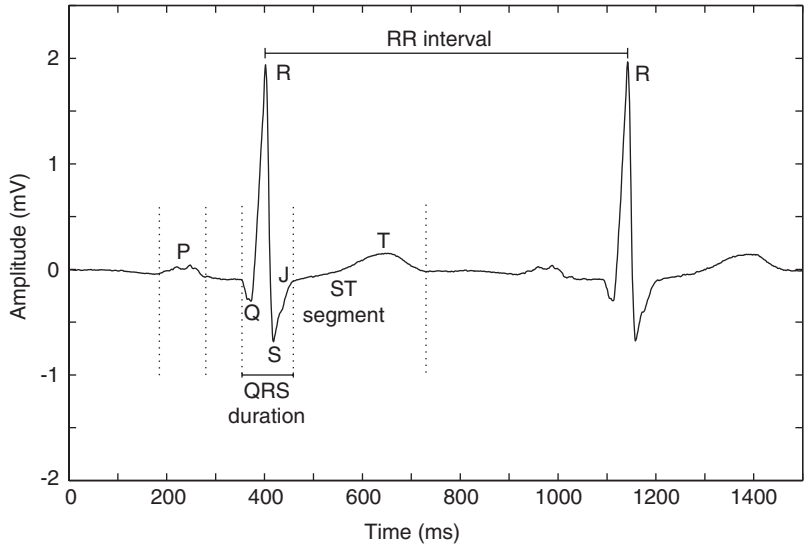

Figure 7. Wave definitions of the cardiac cycle. The onset and end of the P wave, the QRS complex, and the T wave, respectively, are indicated with dotted lines.

values. This type of delineation is illustrated by Fig. 8 where the aim is to find the end of the S wave; the other wave boundaries of the PQRST complex can be found in a similar way. In this example, the search for the endpoint starts when the steepest upslope of the S wave occurs and continues until the derivative of the signal falls below a certain threshold value. The time instant at which the level is crossed defines the QRS end. As the above search procedure is based on the assumption that each of the different waves is present, it is necessary to first establish which waves are absent to ensure meaningful delineation. Such wave detection is usually done by analyzing the pattern of successive peak amplitudes and interpeak distances of the differentiated signal in an interval positioned around the QRS complex.

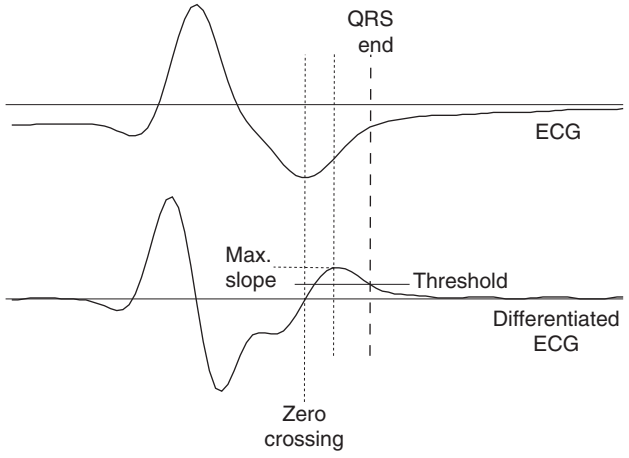

Figure 8. Determination of the QRS end using slope information. The QRS end is the time at which the differentiated signal crosses a threshold after the maximum slope has occurred. The threshold level is usually expressed as a percentage of the maximum slope.

The threshold level that determines the position of a wave boundary may be fixed and chosen with reference to a slope value that is representative of the boundary to be determined. Alternatively, the threshold may be related to signal morphology so that its level is set to a certain percentage of the maximum slope (11). The latter type of thresholding is more suggestive of a cardiologist's approach to delineation because the boundaries of a large-amplitude wave with steep slopes and a low-amplitude wave with less steep slopes will occur at about the same position.

In noisy signals, wave delineation from the differentiated signal performs poorly because an already low signal amplitude at the wave boundary is disturbed by noise. The performance can, to a certain degree, be improved by combining signal differentiation with lowpass filtering to attenuate high-frequency noise. The cut-off frequency of the lowpass filter may be fixed or, better, adapted to the spectral content of the wave to be delineated (12). For example, delineation of the QRS complex should be based on a filter with a higher cut-off frequency than the filter used to find the end of the T wave, reflecting the fact that the T wave contains much less high-frequency components (see Fig. 9).

The threshold levels, or the shapes of the waveform templates, should be chosen such that the resulting delineation agrees with those obtained by cardiological expertise. Following training of the delineation method to obtain suitable parameter values, its performance should be evaluated on a database with P, QRS, and T wave boundaries having been manually annotated (13,14). Delineation performance is described in terms of the mean and standard deviation of the error between the boundaries produced by the method and the experts (15,16). It is

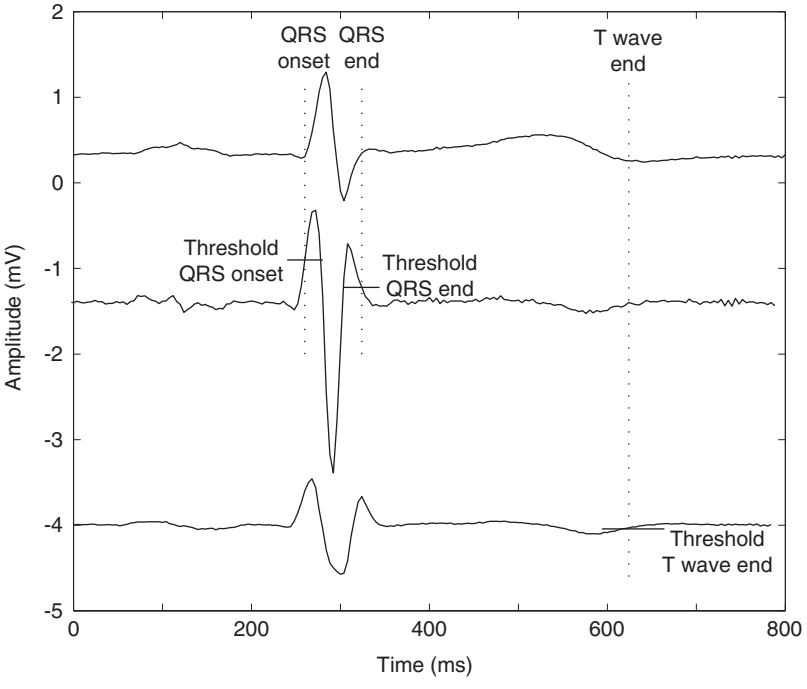

Figure 9. Wave delineation based on lowpass differentiated signals. The original signal (top) is differentiated and lowpass-filtered to yield the QRS onset and end (middle) and the T wave end (bottom). The threshold level that determines each wave boundary is indicated by the horizontal line. A higher cut-off frequency of the lowpass differentiator was used for QRS complex delineation than for the T wave.

important to realize that a zero value of the standard deviation can never be attained because a certain dispersion will always exist even among experts. However, a method's performance is judged as satisfactory when the dispersion is approximately on the same order as that among experts (17).

Wave delineation is particularly problematic when determining the end of the T wave, which is often characterized by a very gradual transition to the isoelectric line of the ECG, see, for example, the T wave in Fig. 9. In fact, its delineation is problematic even among cardiologists, and differences between cardiologists may occasionally approach as much as 100 ms (17). Despite these difficulties, the end of the T wave is an extremely important boundary, required when computing the total duration of ventricular depolarization and repolarization. As a result of the importance of this measurement, several techniques have been developed for the purpose of robustly determining the T wave end (18–20). Multiresolution signal analysis of the ECG using the dyadic wavelet transform, in which the signal is analyzed at different time resolutions, has proven to be well-suited for T wave delineation. By first determining a robust, but preliminary, boundary position from a smooth approximation of the original signal, the position can be refined by analyzing the properties of better approximations in an interval positioned around the preliminary boundary. The wavelet-based approach can, with an appropriate choice of wavelet function, be viewed as a filter bank of lowpass differentiators with varying cut-off frequencies. Evaluating the performance of the methods based on either lowpass differentiation or wavelet analysis, the latter method has been found to produce T wave ends in better agreement with those produced by cardiologists (21).

5. DATA COMPRESSION

As a wide range of clinical examinations involve the recording of ECG signals, huge amounts of data are produced not only for immediate scrutiny, but also for storage in a database for future retrieval and review. It is well-known that the availability of one or several previous ECG recordings improves diagnostic accuracy of various cardiac disorders, including myocardial infarction. Today, such serial ECG comparison encompasses short-duration recordings acquired during rest, but may in the future encompass long signals, for example, acquired during stress testing or ambulatory monitoring. Although hard disk technology has undergone dramatic improvements in recent years, increased disk size is paralleled by the ever-increasing wish of physicians to store more information. In particular, the inclusion of additional ECG leads, the use of higher sampling rates and finer amplitude resolution, the inclusion of other, noncardiac signals such as blood pressure and respiration, and so on, lead to rapidly increasing demands on disk size. It is evident that efficient methods of data compression will be required for a long time to come.

Another driving force behind the development of methods for data compression is the transmission of ECG signals across public telephone networks, cellular networks, intrahospital networks, and wireless communication systems. Such data transmission may be initiated from an ambulance or a patient's home to the hospital and has, among other things, been found to be valuable for early diagnosis of an infarct.

An ECG signal exhibits a certain amount of redundancy, as manifested by correlation between adjacent samples, the recurrence of heartbeats with similar morphology, and the relative resemblance between different leads. Considerable savings can be achieved in terms of storage capacity and transmission time by exploiting the different types of redundancy so that each sample can be represented by fewer bits than in the original signal. Hence, the data compression algorithm should account for the fact that the signal contains recurrent heartbeats, often with similar morphology, and that the signal is, almost invariably, a multilead recording. Equally important, it must account for the fact that both small- and large-amplitude waveforms are present in the signal, carrying important diagnostic information, whereas the isoelectric line contains negligible information.

The overall goal is to represent a signal as accurately as possible using the fewest number of bits, by applying either lossless compression, in which the reconstructed signal is an exact replica of the original signal, or lossy compression, in which the reconstructed signal is allowed to differ from the original signal. With lossy compression, a certain amount of distortion has to be accepted in the reconstructed signal, although the distortion must remain small enough not to modify the diagnostic content of the ECG. For both types of compression, it may be necessary to perform noise filtering of the ECG signal before it is subjected to data compression.

The outcome of data compression is critically dependent on the sampling rate and the number of bits used to represent each sample of the original signal. For example, a signal acquired at a low sampling rate contains less redundancy than one acquired at a high rate; as a result, the compression ratio, defined as the bit size of the original signal divided by the bit size of the compressed signal, is lower for a signal acquired at a lower sampling rate. Other factors that influence the outcome of data compression are the signal bandwidth, the number of leads, and the noise level. For example, a signal sampled at a rate of 500 Hz but bandlimited to 50 Hz is associated with a better compression ratio than is a signal bandlimited to the Nyquist frequency of 250 Hz. Consequently, it is imperative that any comparison of performance for different compression methods is based on identical values of the system parameters.

Methods for data compression may be categorized according to the following three main types of data redundancy found in ECG recordings:

- *Intersample* or, equivalently, *intrabeat* redundancy is exploited by employing either direct or transform-based methods.
- *Interbeat* redundancy is manifested, within each lead, by successive, similar-looking heartbeats.

Hence, their occurrence times must be determined by a QRS detector before interbeat redundancy can be exploited.

- *Interlead* redundancy is because of the fundamental fact that a heartbeat is "viewed" concurrently in different leads. Therefore, waveforms exhibit interlead correlation that depend on the distance between electrodes on the body surface.

It should be noted that many methods of data compression have been designed to solely deal with the first type of redundancy, although methods that deal with all three types combined are becoming increasingly common. The block diagram in Fig. 10 presents the two main steps in data compression. In the first step, the redundancy of the original signal is reduced so that a more compact signal representation is obtained. The output data is then fed to an encoder whose purpose is to produce an efficiently coded bit stream suitable for storage or transmission.

5.1. Direct Methods for Data Compression

Direct methods operate in the time domain by extracting a set of K "significant" samples $x(n_k)$ from the original signal $x(n)$ such that

$$\begin{aligned}&(n,x(n)), n=0,\ldots,N-1 \rightarrow (n_k,x(n_k)),\\ &k=0,\ldots,K-1,\end{aligned} \tag{2}$$

where $K<N$. The resulting subset of K samples is retained for data compression, and the other samples are discarded. Reconstruction of the samples between the significant samples is achieved by interpolation using the following general expression:

$$\tilde{x}(n)=\begin{cases} x(n), & n=n_0,\ldots,n_{K-1};\\ f_{n_0,n_1}(n), & n=n_0+1,\ldots,n_1-1;\\ \vdots & \vdots\\ f_{n_{K-2},n_{K-1}}(n), & n=n_{K-2}+1,\ldots,n_{K-1}-1.\end{cases} \tag{3}$$

The first and last significant samples of the signal $x(n)$ are usually chosen to be $n_0=0$ and $n_{K-1}=N-1$, respectively. The interpolating function $f_{n_{k-1},n_k}(n)$ usually has a polynomial form of low order, approximating the signal with zero- or first-order polynomials, for example, by a sequence of plateaus or straight lines. First-order (linear) interpolation has become especially popular because the signal can be completely reconstructed from the set of significant samples $x(n_k)$. Although more advanced interpolating functions can be used (e.g., rational or trigonometric functions), additional parameters need to be stored as side information to reconstruct the signal. As a result, improvements in performance may still be lost because of the additional cost of representing the interpolating function.

The selection of significant samples can be viewed as an "intelligent" subsampling of the signal in which the isoelectric segments are approximated by a small number of samples, whereas the QRS complex is much more densely sampled so that the essential information contained in the ECG is preserved. A simplistic approach would be to select the significant samples from among the turning points of the signal (i.e., its peaks and valleys); however, the error between the original and reconstructed signal may at times be quite considerable. Therefore, the selection of significant samples is usually based on a criterion assuring that the reconstruction error remains within a certain tolerance. The selection process can be performed sequentially so that the next significant sample is selected with reference to the properties of preceding signal properties. Alternatively, a larger block of samples can be processed at the same time so that significant samples are selected with reference to the enclosing signal properties. Although the block-based approach can be expected to yield better performance, it is less suitable for real-time processing.

The performance of direct methods is particularly influenced by the noise level of the ECG, as the number of significant samples required to meet the maximal error tolerance increases as the noise level increases. Accordingly, poorer compression ratios are achieved at high noise levels. Although direct methods work satisfactorily when processing ECGs acquired during resting conditions, the very idea of selecting significant samples can be questioned in noisy recordings.

AZTEC and SAPA are two well-known examples of direct methods for data compression (22,23); several variations and improvements on these two methods have been suggested over the years (24,25).

5.2. Transform-Based Data Compression

Transform-based compression assumes that a compact signal representation exists in terms of the coefficients of

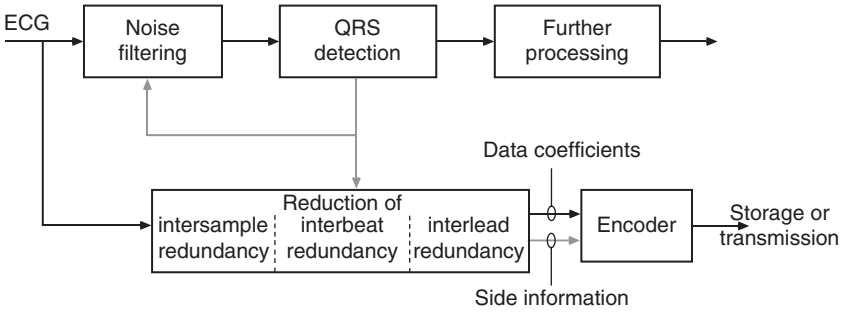

Figure 10. Data compression of ECG signals. The output of the block performing redundancy reduction is a sequence of data coefficients. The output may also include side information, which, for example, describes the set of basis functions used for computing the data coefficients. The encoder translates the input into an efficiently coded bit stream.

a truncated orthonormal expansion,

$$\mathbf{x} = \sum_{k=1}^{N} w_k \boldsymbol{\varphi}_k, \tag{4}$$

where $\mathbf{x}$ denotes a column vector containing N ECG samples, w_k the coefficients, and $\boldsymbol{\varphi}_k$ the basis functions. The basic idea is to obtain an estimate of $\mathbf{x}$ by truncation of the complete series expansion in Equation 4 so that only K out of the N terms are included. The coefficients $w_1, \ldots, w_K$ are retained for storage or transmission, hopefully providing adequate signal reconstruction, whereas the remaining $(N-K)$ coefficients, being near zero, are discarded. The coefficients w_k are obtained by correlating $\mathbf{x}$ with each of the basis functions (i.e., by computing the inner product $w_k = \boldsymbol{\varphi}_k^T \mathbf{x}$). Hence, the subset of K coefficients constitutes the information to be compressed, and from which the signal is later reconstructed. If the basis functions are *a priori* unknown, the set of coefficients must be supplemented with the samples of the required basis functions. Following data compression, the reconstructed signal $\tilde{\mathbf{x}}_K$ is obtained from

$$\tilde{\mathbf{x}}_K = \sum_{k=1}^{K} w_k \boldsymbol{\varphi}_k. \tag{5}$$

In contrast to most direct methods, transform-based methods require that the ECG first be partitioned into a series of successive blocks, where each block is subsequently subjected to data compression. The signal may be partitioned so that each block contains one heartbeat, and, therefore, QRS detection must always precede such compression methods. Each block is positioned around the QRS complex, starting at a fixed distance before the QRS that includes the P wave and extending beyond the T wave end to the beginning of the next beat. As the heart rate is not constant, the distance by which the block extends after the QRS complex is adapted to the prevailing heart rate.

A fixed number of basis functions are often considered for data compression, with the value of K being chosen from considerations concerning overall performance expressed in terms of compression ratio and reconstruction error. Although serving as an important guideline to the choice of K, such an approach may occasionally produce an unacceptable representation of certain beat morphologies. As the loss of morphologic detail causes incorrect interpretation of the ECG, the choice of K can be adapted for every beat to the properties of the reconstruction error $(\mathbf{x} - \tilde{\mathbf{x}}_K)$ (26). For example, the value of K may be chosen such that the RMS value of the reconstruction error does not exceed the error tolerance ε or, more demanding, that none of the reconstruction errors of the entire block exceeds ε. It is evident that the value of K sometimes becomes much larger than the value suggested based on considerations on overall performance; however, it sometimes also becomes smaller. By letting K be variable, one can fully control the quality of the reconstructed signal, while also being forced to increase the amount of side information because one must keep track of the value of K for every data block.

A crucial question to address is which set of basis functions to choose for data compression. It is well-known that the Karhunen–Loève (KL) expansion is optimal in that it minimizes the MSE of approximation, and, therefore, the KL basis functions have become popular (26–28). The basis functions are obtained as eigenvectors of the correlation matrix $\mathbf{R}_x$ that is determined from one or several datasets. The basis functions are labeled "universal," when the dataset originates from many patients, or "subject-specific," when the data originates from a single recording. Although it is rarely necessary to store or transmit universal basis functions, subject-specific functions need to be part of the side information. The use of universal KL basis functions is illustrated by Fig. 11.

The above-mentioned compression methods are designed to reduce intersample redundancy of the ECG, while not dealing with the fact that successive beats often have almost identical morphology. A simplistic approach to dealing with interbeat redundancy is to use the previous beat to predict the next, and to only code the difference. By repeating the prediction for all beats, a difference signal is produced whose magnitude is much smaller than the original one, thus requiring fewer bits for its representation. A major drawback of the simple "previous-beat" predictor is its vulnerability to noise, a property that can be improved by using a predictor based on averaging of the most recent beats (29).

A fundamental assumption of the beat subtraction approach is that the beats, used to predict the next beat, exhibit similar morphology. To ensure this similarity, it is necessary to first categorize the beats according to their respective morphology so that several average beats can be initialized. A straightforward approach to such beat categorization (clustering) would be to consider the energy of the prediction error $\sum_n e_i^2(n)$ in a beat interval: A new average beat is initialized if the energy exceeds a certain threshold, unless the current beat matches an already existing average beat category.

As considerable correlation exists between different ECG leads, data compression of multilead ECGs would benefit from exploring interlead redundancy rather than just applying the previously described methods to one lead at a time. Direct methods for single-lead data compression have turned out to be not easily extended to multilead compression, although a few adaptations have been presented. With transform-based methods, interlead correlation may be dealt with in two steps, namely, a transformation that concentrates the signal energy spread over the total number of leads into a few leads, followed by compression of each transformed lead using a single-lead technique (5).

5.3. Performance Evaluation

The *compression ratio* $\mathscr{P}_{\mathrm{CR}}$ is a crucial measure when evaluating the performance of data compression methods. It is defined as the ratio between the number of bits required to represent the original signal $x(n)$ and the number of bits required to represent the compressed

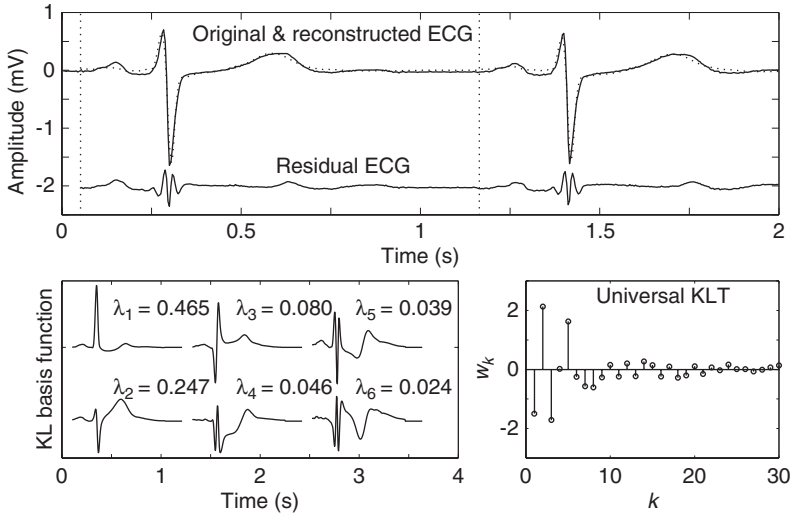

Figure 11. Transform-based data compression using the KL basis functions derived from a huge database including thousands of ECGs from different subjects. The basis functions $\boldsymbol{\varphi}_k$ and associated eigenvalues λ_k are presented, as are the 30 largest coefficients of the original ECG's KL transform. The ECGs are reconstructed with $K = 8$.

signal $\tilde{x}(n)$. Another crucial measure is the *bit rate* $\mathscr{P}_{\mathrm{BR}}$, defined as the average number of bits required per second to represent the ECG, and is, in contrast to $\mathscr{P}_{\mathrm{CR}}$, independent of sampling rate and word length. However, none of these two measures provide sufficient detail on the performance when lossy data compression is used because they do not reflect the distortion of the reconstructed signal. Accordingly, an excellent $\mathscr{P}_{\mathrm{CR}}$ or $\mathscr{P}_{\mathrm{BR}}$ may be achieved at the expense of a severely distorted signal, and, therefore, an essential aspect of data compression is to define complementary performance measures that reflect the accuracy with which the diagnostic information in the original ECG signal is preserved.

The percentage root mean-square difference (PRD) is a frequently employed distortion measure that quantifies the error between the original signal $x(n)$ and the reconstructed $\tilde{x}(n)$, defined by

$$\mathscr{P}_{\mathrm{PRD}} = 100 \cdot \sqrt{\sum_{n=0}^{N-1} (x(n) - \tilde{x}(n))^2 \Big/ \sum_{n=0}^{N-1} x^2(n)}, \qquad (6)$$

where it is assumed that the mean value of $x(n)$ has been subtracted prior to data compression. The measure $\mathscr{P}_{\mathrm{PRD}}$ has become popular because of its computational simplicity and the ease with which distortion can be compared from one signal to another. However, $\mathscr{P}_{\mathrm{PRD}}$ has certain flaws that make it unsuitable for performance evaluation. For example, compression of ECGs with large-amplitude QRS complexes results in less distortion than does compression of an ECG with small-amplitude QRS complexes, even if the squared error $(x(n) - \tilde{x}(n))^2$ is identical in both cases. This disadvantage can, to a certain degree, be mitigated by replacing the energy normalization in $\mathscr{P}_{\mathrm{PRD}}$ with a fixed normalization so that the modified measure, denoted $\mathscr{P}_{\mathrm{RMS}}$, describes the error in absolute terms,

$$\mathscr{P}_{\mathrm{RMS}} = \sqrt{\frac{1}{N} \sum_{n=0}^{N-1} (x(n) - \tilde{x}(n))^2}. \qquad (7)$$

This measure is somewhat more suggestive of diagnostic ECG interpretation where criteria are expressed as millivolt wave amplitudes rather than in percentages of signal energy. However, care should be exercised when noisy signals are compressed because $\mathscr{P}_{\mathrm{RMS}}$ then would represent the noise discarded by the compression method, as measured by the difference between $x(n)$ and $\tilde{x}(n)$, rather than by the distortion of the ECG.

Performance is often presented as a rate distortion curve where signal distortion is displayed as a function of $\mathscr{P}_{\mathrm{BR}}$. Such a curve is shown in Fig. 12 for transform-based data compression (based on the KL transform), with $\mathscr{P}_{\mathrm{RMS}}$ as the chosen distortion measure. With this type of curve, the operating point of a compression method can be easily defined, specifying the bit rate at which acceptable distortion of the reconstructed signal is achieved. By

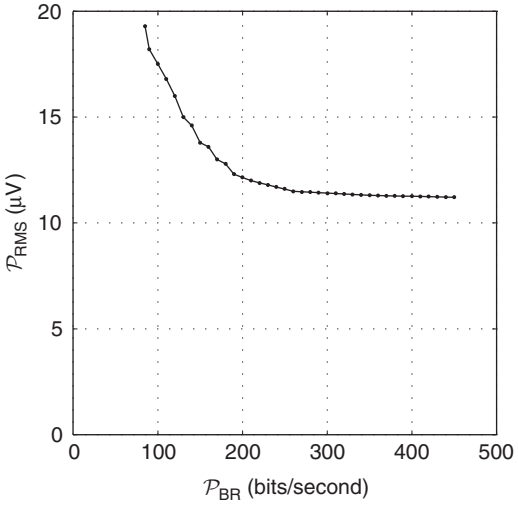

Figure 12. Rate distortion curves for data compression based on the KL transform, where account is taken of the required side information when calculating $\mathscr{P}_{\mathrm{BR}}$. The results were obtained from 10 minutes of ECG data, selected from the MIT–BIH database.

requiring the distortion to be low, for example, a $\mathscr{P}_{\mathrm{RMS}}$ of only 12 μV, it is tempting to believe that the diagnostic information in the reconstructed signal is preserved. However, both $\mathscr{P}_{\mathrm{PRD}}$ and $\mathscr{P}_{\mathrm{RMS}}$ suffer from an inability to reflect loss of diagnostic information; instead, all samples are treated equally whether located in the QRS complex or in the uninformative isoelectric segment. Although the loss of a tiny Q wave in the reconstructed signal essentially goes unreflected, the absence of a Q wave represents an essential loss from a diagnostic point of view when, for example, diagnosing myocardial infarction.

The weighted diagnostic distortion (WDD) measure $\mathscr{P}_{\mathrm{WDD}}$ is one of the few mathematically defined measures that addresses the limitations of distortion measures based on the error between samples of the original and reconstructed signal (30). The measure $\mathscr{P}_{\mathrm{WDD}}$ is composite because it involves various wave parameters essential to ECG interpretation, especially wave amplitudes and durations of the PQRST complex. Assuming that measurements of the kth ECG parameter have been obtained from the original and reconstructed signals, denoted β_k and $\tilde{\beta}_k$ respectively, a normalized error $\Delta\beta_k$ can be defined,

$$\Delta\beta_k = \frac{|\beta_k - \tilde{\beta}_k|}{\max(|\beta_k|, |\tilde{\beta}_k|)}, \tag{8}$$

which is constrained to the interval $0 < \Delta\beta_k \leq 1$; it is assumed that β_k and $\tilde{\beta}_k$ have nonzero values. When several beats are available for measurement, the resulting values of $\Delta\beta_k$ are averaged before further processing is done. For a set of P different parameters on amplitude and duration, the WDD performance measure is defined as

$$\mathscr{P}_{\mathrm{WDD}} = 100 \cdot \sum_{k=1}^{P} \alpha_k (\Delta\beta_k)^2 \Bigg/ \sum_{k=1}^{P} \alpha_k, \tag{9}$$

where the coefficients α_k make it possible to weight the parameter measurement errors $\Delta\beta_k$ in relation to their overall significance. Such weighting can be used to emphasize measurements of particular significance, such as ST segment measurements in ischemia monitoring.

An important aspect of performance evaluation is, of course, the choice of ECG database. As the performance of a method depends on the noise level, the evaluation should be based on data representative of the application in question. The amount of ectopic beats and arrhythmias are other factors that, to various degrees, influence the evaluation outcome.

6. CLUSTERING OF BEAT MORPHOLOGIES

Feature extraction may be performed for the purpose of characterizing the morphology of a QRS complex. Although the durations and amplitudes that result from wave delineation contain important diagnostic information, additional features are required to reliably group beats with similar morphology into the same cluster. One approach to feature extraction is to derive a set of "heuristic" features that, for example, describe the area, polarity, and slopes of the waves. Another, more robust, approach is to make use of the coefficients that result from the correlation of each beat with either a set of predefined orthonormal basis functions or a set of QRS templates. Based on the set of extracted features, clustering of QRS morphologies can be performed. In its simplest form, clustering may be used to single out beats that deviate from the predominant morphology, which is usually that belonging to the normal sinus beat (see Fig. 13). Once this is done, beats belonging to the "sinus cluster" can be subjected to, for example, ensemble averaging or heart rate variability analysis. In other situations, reason to study the entire range of beat clusters exists. As clustering does not assign a label with a physiological meaning to a beat, it may be necessary to classify the beats according to their cardiac origin.

Clustering is based on a set of features, contained in the column vector $\mathbf{p}_i$, which describe waveform morphology and, possibly, also rhythm properties of the current beat. In its simplest form, $\mathbf{p}_i$ contains time-domain samples of the QRS samples, and is often used in combination with the cross-correlation coefficient ρ_{il} as a measure of pattern similarity (31–34),

$$\rho_{il} = \frac{\mathbf{p}_i^T \boldsymbol{\mu}_l}{\| \mathbf{p}_i \|_2 \| \boldsymbol{\mu}_l \|_2}, \tag{10}$$

where $\| \cdot \|_2$ denotes the Euclidean norm. The column vector $\boldsymbol{\mu}_l$ defines the mean of the lth beat cluster (and is commonly referred to as a "template" beat). The ECG samples of the current beat are usually bandpass-filtered before clustering so that the influence of baseline wander and EMG noise is reduced. A straightforward approach to clustering is given by assigning the ith beat to the cluster for which the highest correlation coefficient is achieved, provided that it exceeds a certain minimum threshold; if it does not, a new cluster is created. More advanced approaches to clustering have recently been presented that make use of artificial neural networks, see, for example, Refs. 35 and 36.

Using the cross-correlation coefficient as a measure of similarity, it is easily shown that clustering becomes invariant to changes in QRS amplitude. Amplitude invariance is acceptable in certain types of ECG analysis where the information in demand is restricted to the timing of sinus beats. However, invariance to amplitude changes exceeding those induced by respiration is undesirable when the purpose is to average the sinus beats of a cluster for noise reduction as required, for example, in high-resolution ECG analysis; averaging of similar-shaped beats with widely differing QRS amplitudes produces a nonrepresentative ensemble average.

The basis function representation, previously considered for data compression, has also been considered for feature extraction when clustering heartbeats, often expressed in terms of the Karhunen–Loève or the Hermite basis functions (35–39). In such cases, the coefficients of the series expansion that correspond to the most important basis functions would define the feature vector $\mathbf{p}_i$.

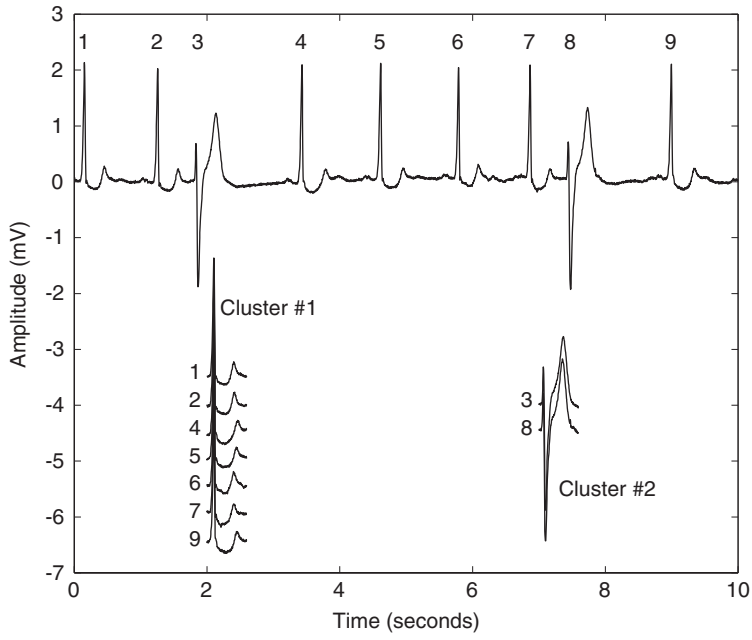

Figure 13. Clustering of an ECG that contains two different beat morphologies. Cluster 1 contains the sinus beats, whereas cluster 2 contains the two ectopic beats.

Improved accuracy of the occurrence time is intimately related to the clustering process because the current beat $\mathbf{p}_i$ can be optimally aligned in time to $\boldsymbol{\mu}_1$ when similarity is measured. The availability of morphologic information through $\boldsymbol{\mu}_1$ may be used to improve the accuracy of the time, originally determined by the QRS detector that operates at a lower temporal resolution (and determined without considering the morphology of previous beats). When clustering is based on the cross-correlation coefficient, the samples of $\mathbf{p}_i$ are correlated to the mean of the cluster $\boldsymbol{\mu}_1$ and shifted in time until the highest cross-correlation value is obtained; the resulting value is used for cluster assignment. It is important to realize that omission of the time alignment operation leads to the initiation of undesired clusters.

7. ECG SIGNAL PROCESSING IN APPLICATIONS

Numerous types of ECG analysis have been developed that draw on the ECG signal processing so far presented. It is outside the scope of this text to provide a comprehensive description of such types of analysis. Instead, this article is concluded by briefly mentioning two types of analyses that both exploit low-level activities of the ECG, aiming either at characterizing static properties of the ECG ("high-resolution ECG") or dynamic properties ("T wave alternans").

7.1. High-Resolution ECG

For many years, the interpretation of resting ECGs was based on measurements derived from waves whose amplitude were at least several tens of microvolts; waves with smaller amplitudes were ignored because these were almost always caused by noise. This limitation was, however, removed with the advent of the high-resolution ECG with which it became possible to detect signals on the order of 1 μV thanks to signal averaging techniques. The high-resolution ECG has helped unlock novel information and has demonstrated that signal processing for the purpose of noise reduction is a clinically viable technique. The acquisition procedure is usually the same as for the resting ECG, except that the signal is recorded over an extended time period so that a sufficiently low noise level is attained by averaging.

Different subintervals of the cardiac cycle have received special attention in high-resolution ECG analysis, and low-level signals have been considered in connection with (1) the bundle of His that depolarizes during the PR segment (40,41), (2) the terminal part of the QRS complex and the ST segment where so-called "late potentials" may be present (42–44), (3) intra-QRS potentials (45,46), and (4) the P wave (47,48). Of these four applications, the analysis of late potentials has received the most widespread clinical attention. Late potentials may be found in patients with myocardial infarction where ventricular depolarization can terminate many milliseconds after the end of the QRS complex (Fig. 14). This prolongation is because of delayed and fragmented depolarization of the cells in the myocardium that surround the dead region (scarred tissue) caused by infarction; the conduction capability of the bordering cells is severely impaired by infarction. Many studies have demonstrated the importance of late potentials when, for example, identifying postinfarct patients at high risk of future life-threatening arrhythmias, see, for example, Ref. 49.

The high-resolution ECG rests on the assumption that the signal to be estimated has a fixed beat-to-beat morphology. As the high-resolution ECG is often expected to contain high-frequency components up to at least 250 Hz, the sampling rate is at least 1 kHz. It is essential that the occurrence time of each beat (the "fiducial point") is accurately determined from each individual beat before

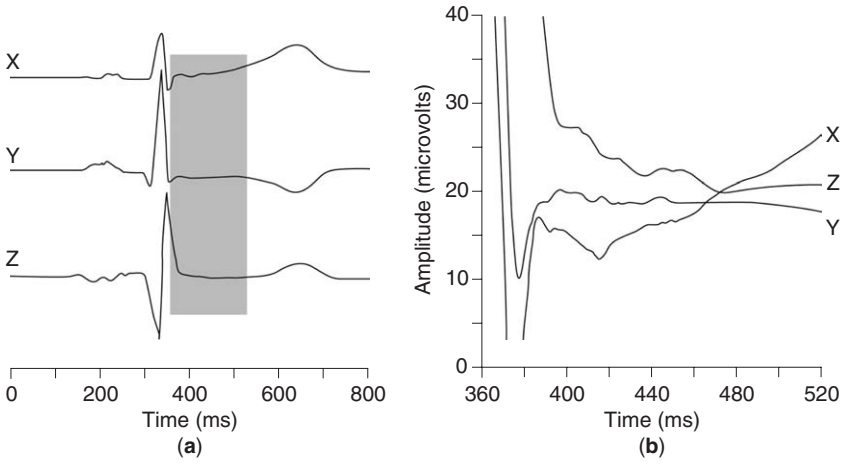

Figure 14. (a) The high-resolution ECG obtained by signal averaging the orthogonal *X*, *Y*, and *Z* leads. (b) The terminal part of the QRS complex and the ST segment (i.e., the interval shaded gray in (a), is magnified 10 times in amplitude to better display the small undulations known as late potentials).

ensemble averaging to avoid smearing of low-amplitude, high-frequency components of the ECG.

Ensemble averaging is related to the following signal model in the ith beat $\mathbf{x}_i$ is assumed to be additively composed of a deterministic signal component $\mathbf{s}$ and random noise $\mathbf{v}_i$, which is asynchronous to cardiac activity,

$$\mathbf{x}_i = \mathbf{s} + \mathbf{v}_i, \quad i = 1, \ldots, M. \tag{11}$$

It is assumed that only sinus beats are modeled (i.e., beats of ectopic origin have already been sorted out by means of some technique for morphologic clustering). Representing the entire ensemble with the matrix $\mathbf{X}$,

$$\mathbf{X} = [\mathbf{x}_1 \ \mathbf{x}_2 \ \cdots \mathbf{x}_M], \tag{12}$$

where each column vector contains one beat, an estimate of the signal $\mathbf{s}$ is obtained by computing the ensemble average,

$$\hat{\mathbf{s}} = \frac{1}{M}\mathbf{X}\mathbf{w}, \tag{13}$$

where $\mathbf{w}$ denotes a weight vector whose elements are all equal to one. When the noise is uncorrelated from beat to beat and with a standard deviation that remains constant throughout the ensemble, the noise level is reduced by a factor $\sqrt{M}$. In situations when the noise level varies over time, it is instead preferable to use weighted averaging in which each weight of $\mathbf{w}$ is inversely proportional to the noise level (5).

Once a low-noise ECG signal is produced by ensemble averaging, the late potential components can be elucidated from the terminal part of the QRS complex and the ST segment using linear, time-invariant highpass filtering. In order to avoid that filter ringing may obscure the low-amplitude components, the ensemble average $\hat{\mathbf{s}}$ is filtered backward in time rather than forward as is customary. The detection of late potentials is commonly accomplished by first determining the time instant when the signal activity ends, involving a threshold procedure that relates to the residual noise level of $\hat{\mathbf{s}}$ (44); then, the amplitude of the interval immediately preceding the determined endpoint must be sufficiently low for a detection to occur.

7.2. T-Wave Alternans

Tiny beat-to-beat alternations in T wave morphology are related to myocardial ischemia and have been found useful as a predictor of malignant ventricular arrhythmias that often lead to sudden cardiac death (50,51). The morphologic alternations follow a flip-flop pattern in which every other T wave has the same morphology (see Fig. 15). The alternans is often a low-amplitude phenomenon in the microvolt range; therefore, it cannot be easily perceived by the naked eye from a standard ECG printout, but requires signal processing techniques for its detection and quantification (52).

Similar to the detection of late potentials, it is crucial that successive T waves are properly aligned in time so that the alternans relates to underlying physiology rather than to inaccurate alignment. On the other hand, ensemble averaging cannot play a central role in detecting T wave alternans as such an operation would obliterate the alternating behavior. Of the several detection methods that have been devised, the most popular detectors are based on the following statistical model of the T wave. At a certain predefined time instant within each T wave, the observed amplitude $x(i)$ is modeled by

$$x(i) = A + a(-1)^i + v(i), \quad i = 1, \ldots, M, \tag{14}$$

where i denotes beat index, M denotes total number of beats, A denotes T wave amplitude, and a denotes alternans amplitude (although it is $2a$ that has physiological significance because it describes the difference between two beats). The additive noise $v(i)$ is assumed to be a zero-mean, random process that is stationary and white. As the amplitude A does not convey any information on alternans, its influence is typically removed from $x(i)$ by subtracting the mean value $\bar{x}$ of $x(1), \ldots, x(M)$ so that the corrected signal $y(i) = x(i) - \bar{x}$ is instead analyzed.

By applying statistical detection theory to the model in Equation 14 under the assumption that the noise $v(i)$

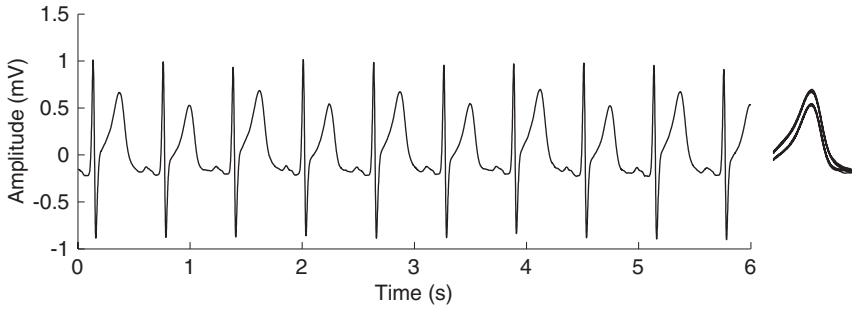

Figure 15. An example of T wave alternans. The alternating behavior between two different T wave morphologies is particularly evident when all T waves are aligned in time and superimposed.

obeys a Gaussian probability density function, it can be shown that the optimal detector performs a correlation between $y(i)$ and the alternating pattern $(-1)^i$, for example:

$$T_G = \left(\sum_{i=1}^{M} y(i)(-1)^i \right)^2 . \tag{15}$$

The M successive T waves are judged to contain alternans when the decision statistic T_G exceeds a certain threshold value. Interestingly, the detector in Equation 15 can be interpreted in terms of power spectral analysis because T_G is exactly the periodogram computed for the highest normalized frequency at 0.5. In fact, one of the most popular detectors was heuristically developed from the observation that alternans is manifested by an increase in spectral power at 0.5 (53); alternans was detected when the power at this frequency exceeded a certain factor of the surrounding spectral power.

The Gaussian detector in Equation 15 is sensitive to the presence of outliers in $y(i)$ caused by, for example, baseline wander and ectopic beats. By assuming instead that the noise $v(i)$ obeys a Laplacian probability density function (i.e., with heavier tails than the Gaussian function), the optimal detector becomes more robust to impulsive noise. In the Laplacian detector, the following decision statistic is compared with a threshold (52),

$$T_L = \sum_{i=1}^{M} (|y(i)(-1)^i| - |y(i)(-1)^i - \hat{a}|), \tag{16}$$

where $\hat{a}$ denotes the maximum likelihood estimator of the alternans amplitude, being defined by

$$\hat{a} = \text{median}(y(1) \cdot (-1), y(2) \cdot 1, \ldots, y(M) \cdot (-1)^M). \tag{17}$$

It is evident from Equation 16 that the Laplacian detector puts less emphasis on large-amplitude values in $y(i)$ than does the Gaussian detector in Equation 15, replacing the squaring operation with absolute values. Moreover, the alternans amplitude a is robustly estimated by computing the median of the signal $y(i)(-1)^i$.

Although the above detectors are designed to process a single interval, they can be easily extended to process intervals defined by a sliding window with the detection procedure repeated in each new interval. With the sliding window approach, a series of successive alternans amplitudes can be produced, thereby providing means for characterizing the morphology of the "alternans waveform."

Using simulated ECG signals, the Laplacian detector has been found to perform better than the Gaussian one (52,54). In general, performance assessment is difficult to study on ECG recordings because manual annotation of T wave alternans episodes cannot be performed because of their low amplitude. However, the use of simulated signals has been found valuable because the presence and extent of T wave alternans can be controlled in detail.

BIBLIOGRAPHY

1. P. W. Macfarlane and T. D. W. Lawrie, eds., *Comprehensive Electrocardiology. Theory and Practice in Health and Disease*, *vols. 1*, *2*, *3*. New York: Pergamon Press, 1989.
2. J. J. Bailey, A. S. Berson, A. Garson, L. G. Horan, P. W. Macfarlanc, D. W. Mortara, and C. Zywictz, Recommendations for the standardization and specifications in automated electrocardiography: bandwidth and signal processing. *Circulation* 1990; **81**:730–739.
3. J. A. van Alsté, W. van Eck, and O. E. Herrman, ECG baseline wander reduction using linear phase filters. *Comput. Biomed. Res.* 1986; **19**:417–427.
4. L. Sörnmo, Time-variable digital filtering of ECG baseline wander. *Med. Biol. Eng. Comput.* 1993; **31**:503–508.
5. L. Sörnmo and P. Laguna, *Bioelectrical Signal Processing in Cardiac and Neurological Applications*. Amsterdam: Elsevier (Academic Press), 2005.
6. J. C. Huhta and J. G. Webster, 60-Hz interference in electrocardiography. *IEEE Trans. Biomed. Eng.* 1973; **43**:91–101.
7. C. D. McManus, D. Neubert, and E. Cramer, Characterization and elimination of AC noise in the electrocardiogram: a comparison of digital filtering methods. *Comput. Biomed. Res.* 1993; **26**:48–67.
8. P. S. Hamilton, A comparison of adaptive and nonadaptive filters for the reduction of powerline interference in the ECG. *IEEE Trans. Biomed. Eng.* 1996; **43**:105–109.
9. O. Pahlm and L. Sörnmo, Software QRS detection in ambulatory monitoring—a review. *Med. Biol. Eng. Comput.* 1984; **22**:289–297.
10. B-U. Köhler, C. Hennig, and R. Orglmeister, The principles of software QRS detection. *IEEE Eng. Med. Biol. Mag.* 2002; **21**:42–57.
11. P. Laguna, R. Jané, and P. Caminal, Automatic detection of wave boundaries in multilead ECG signals: validation with the CSE database. *Comput. Biomed. Res.* 1994; **27**:45–60.

12. P. Laguna, N. V. Thakor, P. Caminal, and R. Jané, Low-pass differentiators for biological signals with known spectra: application to ECG signal processing. *IEEE Trans. Biomed. Eng.* 1990; **37**:420–424.
13. J. L. Willems, P. Arnaud, J. H. van Bemmel, P. J. Bourdillon, R. Degani, B. Denis, I. Graham, F. M. A. Harms, P. W. Macfarlane, G. Mazzocca, J. Meyer, and C. Zywietz, A reference data base for multi-lead electrocardiographic computer measurement programs. *J. Am. Coll. Cardiol.* 1987; **10**:1313–1321.
14. P. Laguna, R. G. Mark, A. L. Goldberger, and G. B. Moody, A database for evaluation of algorithms for measurement of QT and other waveform intervals in the ECG. *Proc. Computers in Cardiology*, IEEE Press, 1997:673–676.
15. J. L. Willems, P. Arnaud, J. H. van Bemmel, et al., Assessment of the performance of electrocardiographic computer program with the use of a reference data base. *Circulation* 1985; **71**:523–534.
16. R. Jané, A. Blasi, J. García, and P. Laguna, Evaluation of an automatic detector of waveform limits in Holter ECGs with the QT database. *Proc. Computers in Cardiology*, IEEE Press, 1997:295–298.
17. The CSE Working Party, Recommendations for measurement standards in quantitative electrocardiography. *Eur. Heart J.* 1985; **6**:815–825.
18. J. H. van Bemmel, C. Zywietz, and J. A. Kors, Signal analysis for ECG interpretation. *Methods Inf. Med.* 1990; **29**:317–329.
19. Q. Xue and S. Reddy, Algorithms for computerized QT analysis. *J. Electrocardiol.* 1998; **30**:181–186.
20. B. Acar, G. Yi, K. Hnatkova, and M. Malik, Spatial, temporal and wavefront direction characteristics of 12-lead T-wave morphology. *Med. Biol. Eng. Comput.* 1999; **37**:574–584.
21. J. P. Martínez, R. Almeida, S. Olmos, A. P. Rocha, and P. Laguna, A wavelet-based ECG delineator: Evaluation on standard databases. *IEEE Trans. Biomed. Eng.* 2004; **51**:570–581.
22. J. R. Cox, F. M. Nolle, H. A. Fozzard, and G. C. Oliver, AZTEC, a preprocessing program for real time ECG rhythm analysis. *IEEE Trans. Biomed. Eng.* 1968; **15**:128–129.
23. M. Ishijima, S-B. Shin, G. H. Hostetter, and J. Sklansky, Scan-along polygonal approximation for data compression of electrocardiograms. *IEEE Trans. Biomed. Eng.* 1983; **30**:723–729.
24. S. M. S. Jalaleddine, C. G. Hutchens, R. D. Strattan, and W. A. Coberly, ECG data compression techniques: a unified approach. *IEEE Trans. Biomed. Eng.* 1990; **37**:329–343.
25. D. Haugland, J. Heber, and J. Husøy, Optimisation algorithms for ECG data compression. *Med. Biol. Eng. Comput.* 1997; **35**:420–424.
26. T. Blanchett, G. C. Kember, and G. A. Fenton, KLT-based quality controlled compression of single-lead ECG. *IEEE Trans. Biomed. Eng.* 1998; **45**:942–945.
27. N. Ahmed, P. J. Milne, and S. G. Harris, Electrocardiographic data compression via orthogonal transforms. *IEEE Trans. Biomed. Eng.* 1975; **22**:484–487.
28. M. E. Womble, J. S. Halliday, S. K. Mitter, M. C. Lancaster, and J. H. Triebwasser, Data compression for storing and transmitting ECG's/VCG's. *Proc. IEEE* 1977; **65**:702–706.
29. P. S. Hamilton and W. J. Tompkins, Compression of the ambulatory ECG by average beat subtraction and residual differencing. *IEEE Trans. Biomed. Eng.* 1991; **38**:253–259.
30. Y. Zigel, A. Cohen, and A. Katz, The weighted diagnostic distortion (WDD) measure for ECG signal compression. *IEEE Trans. Biomed. Eng.* 2000; **47**:1422–1430.
31. G. J. Balm, Crosscorrelation techniques applied to the electrocardiogram interpretation problem. *IEEE Trans. Biomed. Eng.* 1967; **14**:258–262.
32. C. L. Feldman, P. G. Amazeen, M. D. Klein, and B. Lown, Computer detection of ectopic beats. *Comput. Biomed. Res.* 1971; **3**:666–674.
33. J. H. van Bemmel and S. J. Hengevald, Clustering algorithm for QRS and ST–T waveform typing. *Comput. Biomed. Res.* 1973; **6**:442–456.
34. M. E. Nygårds and J. Hulting, An automated system for ECG monitoring. *Comput. Biomed. Res.* 1979; **12**:181–202.
35. Y. H. Hu, S. Palreddy, and W. J. Tompkins, A patient-adaptable ECG beat classifier using a mixture of experts approach. *IEEE Trans. Biomed. Eng.* 1997; **44**:891–900.
36. M. Lagerholm, C. Peterson, G. Braccini, L. Edenbrandt, and L. Sörnmo, Clustering ECG complexes using Hermite functions and self-organizing maps. *IEEE Trans. Biomed. Eng.* 2000; **47**:838–848.
37. T. Y. Young and W. H. Huggins, On the representation of electrocardiograms. *IEEE Trans. Biomed. Eng.* 1963; **10**:86–95.
38. A. R. Hambley, R. L. Moruzzi, and C. L. Feldman, The use of intrinsic components in an ECG filter. *IEEE Trans. Biomed. Eng.* 1974; **21**:469–473.
39. P. Laguna, R. Jané, S. Olmos, N. V. Thakor, H. Rix, and P. Caminal, Adaptive estimation of QRS complex by the Hermite model for classification and ectopic beat detection. *Med. Biol. Eng. Comput.* 1996; **34**:58–68.
40. E. J. Berbari, R. Lazzara, P. Samet, and B. J. Scherlag, Noninvasive techniques for detection of electrical activity during the P-R segment. *Circulation* 1973; **148**:1005–1013.
41. N. C. Flowers, R. C. Hand, P. C. Orander, C. B. Miller, M. O. Walden, and L. G. Horan, Surface recording of electrical activity from the region of the bundle of His. *Am. J. Cardiol.* 1974; **33**:384–389.
42. M. B. Simson, Use of signals in the terminal QRS complex to identify patients with ventricular tachycardia after myocardial infarction. *Circulation* 1981; **64**:235–242.
43. E. J. Berbari, High resolution electrocardiography. *CRC Crit. Rev.* 1988; **16**:67–103.
44. E. J. Berbari and P. Lander, Principles of noise reduction. In: N. El-Sherif, and G. Turitto, eds., *High-Resolution Electrocardiography*. Armonk: Futura Publications, 1992, pp. 51–66.
45. S. Abboud, Subtle alterations in the high-frequency QRS potentials during myocardial ischemia in dogs. *Comput. Biomed. Res.* 1987; **20**:384–395.
46. P. Lander, P. Gomis, R. Goyal, E. J. Berbari, P. Caminal, R. Lazzara, and J. S. Steinberg, Improved predictive value for arrhythmic events using the signal-averaged electrocardiogram. *Circulation* 1997; **95**:1386–1393.
47. M. Fukunami, T. Yamada, M. Ohmori, K. Kumagai, K. Umemoto, A. Sakai, N. Kondoh, T. Minamino, and N. Hoki, Detection of patients at risk for paroxysmal atrial fibrillation during sinus rhythm by P wave-triggered signal-averaged electrocardiogram. *Circulation* 1991; **83**:162–169.
48. J. S. Steinberg, S. Zelenkofske, S. C. Wong, M. Gelernt, R. Sciacca, and E. Menchavez, Value of the P-wave signal-averaged ECG for predicting atrial fibrillation after cardiac surgery. *Circulation* 1992; **88**:2618–2622.

49. M. B. Simson and P. W. Macfarlane, The signal-averaged electrocardiogram. In: P. W. Macfarlane, and T. D. W. Lawrie, eds., *Comprehensive Electrocardiology. Theory and Practice in Health and Disease, vol. 2*. New York: Pergamon Press, 1989, pp. 1199–1218.

50. D. R. Adam, J. M. Smith, S. Akselrod, S. Nyberg, A. O. Powell, and R. J. Cohen, Fluctuations in T-wave morphology and susceptibility to ventricular fibrillation. *J. Electrocardiol*. 1984; **17**:209–218.

51. D. S. Rosenbaum, L. E. Jackson, J. M. Smith, H. Garan, J. N. Ruskin, and R. J. Cohen, Electrical alternans and vulnerability to ventricular arrhythmias. *N. Engl. J. Med*. 1994; **330**:235–241.

52. J. P. Martínez and S. Olmos, Methodological principles of T wave alternans analysis: a unified framework. *IEEE Trans. Biomed. Eng.* 2005; **52**:599–613.

53. J. M. Smith, E. A. Clancy, R. Valeri, J. N. Ruskin, and R. J. Cohen, Electrical alternans and cardiac electrical instability. *Circulation* 1988; **77**:110–121.

54. B. D. Nearing and R. L. Verrier, Modified moving average analysis of T-wave alternans to predict ventricular fibrillation with high accuracy. *J. Appl. Physiol.* 2002; **92**:541–549.